

Doping of the nanocrystalline semiconductor zinc oxide with the donor indium

Th. Agne,^{a)} Z. Guan, X. M. Li, H. Wolf, and Th. Wichert

Technische Physik, Universität des Saarlandes, D-66041 Saarbrücken, Germany

H. Natter and R. Hempelmann

Physikalische Chemie, Universität des Saarlandes, D-66041 Saarbrücken, Germany

(Received 25 April 2003; accepted 6 June 2003)

Doping of the nanocrystalline semiconductor ZnO with the donor ¹¹¹In was achieved by the incorporation of ¹¹¹In atoms during the growth process followed by a hydrothermal treatment at 473 K. The incorporation of ¹¹¹In on substitutional Zn sites was shown by the perturbed $\gamma\gamma$ angular correlation technique. The structural quality of nanocrystalline ZnO with a mean grain size of 11 nm is significantly improved by annealing at 473 K, as revealed by x-ray diffraction, transmission electron microscopy, optical absorption measurements, and photoluminescence spectroscopy. It is shown that the incorporation of ¹¹¹In on undisturbed Zn sites in nanocrystalline ZnO seems to be supported by the onset of crystal growth and by the removal of intrinsic defects. © 2003 American Institute of Physics. [DOI: 10.1063/1.1598289]

Among the current research on nanocrystalline materials, there are extensive investigations of nanometer-scale semiconductors, which exhibit strongly size-dependent optical and electrical properties.¹ However, the doping of nanocrystalline semiconductors, a procedure that forms the basis for the success of semiconductor technology still poses a severe problem in these materials.² Most effort for solving this problem has focused on II-VI semiconductor nanocrystals doped with impurities, such as Mn and Cu, or rare-earth elements, such as Tb (see Refs. 10–13 in Ref. 2).

Here, we report on the doping of the nanocrystalline II-VI semiconductor ZnO (nano-ZnO), which was achieved by introducing In atoms during growth followed by a hydrothermal treatment at 473 K. This procedure led to a volume-weighted mean grain size of 11 nm. The experiments indicate the incorporation of the dopant In as a potential shallow donor on substitutional Zn sites. The incorporation of In atoms on the Zn site, which is a prerequisite for the formation of a shallow donor state, was determined from measurements of the electric field gradient at the site of the dopant atoms. The quality of the undoped nanocrystallites, that is, crystallinity, size, and size distribution, was determined by x-ray diffraction (XRD), transmission electron microscopy (TEM), optical absorption measurements, and photoluminescence spectroscopy (PL). First results on the incorporation of In in nano-ZnO were obtained after annealing at 573 K in a furnace,³ but the volume-weighted mean grain size of the annealed sample was about 20 nm,⁴ so that the optical experiments did not show any confinement effects, such as a shift of the band gap.

Nano-ZnO was produced by the electrochemical deposition under oxidizing conditions (EDOC) method.^{3,4} The electrolysis process uses two Zn electrodes and takes place in a solution of 0.1-M tetrabutylammonium-bromide (TBA-Br) dissolved in 2-propanol. Before growth, high-purity zinc

foils were etched in a solution of 37% HCl for 60 s and subsequently rinsed in an ultrasonic bath in bidistilled water and in 2-propanol. For the electrolysis, a current density of 10 mA/cm² was applied at a temperature of about 303 K. The nano-ZnO crystallites were doped *in situ* with In atoms by diffusing radioactive ¹¹¹In atoms before electrolysis from a dried ¹¹¹InCl₃ solution into the sacrificial electrode. By measuring the radioactivity of the produced nano-ZnO the relative concentration of ¹¹¹In was estimated to 1 ppb. Typically an amount of 100 mg nano-ZnO was produced during a single run; but the EDOC method can easily be upscaled for the production of larger quantities.⁴ During this procedure, the clusters are coated with TBA, which works as a stabilizer of the colloidal nanocrystallites. For the hydrothermal treatment the ZnO nanocrystals were dissolved in 2-propanol and the solution, encapsulated into a pressure vessel, was heated at a temperature between 373 and 523 K. At the maximum temperature of 523 K, the pressure in the vessel was about 8.2 MPa.

In ZnO, the incorporation of the ¹¹¹In atoms on Zn sites can easily be established by comparing the electric field gradient (EFG), measured at the site of the radioactive dopant ¹¹¹In/¹¹¹Cd in a perturbed $\gamma\gamma$ angular correlation experiment (PAC),⁵ with the well-known EFG caused by the hexagonal ZnO lattice at the Zn site. Choosing V_{zz} as the largest component of the traceless EFG tensor (i.e., $V_{xx} + V_{yy} + V_{zz} = 0$) and the asymmetry parameter $\eta = (V_{xx} - V_{yy})/V_{zz}$, the EFG measured by the probe ¹¹¹In/¹¹¹Cd in bulk ZnO is characterized by the coupling constant $\nu_Q = eQV_{zz}/h = 31.2(1)$ MHz and $\eta = 0$;⁶ here, Q is the nuclear quadrupole moment of the isomeric 245-keV $-5/2^+$ level of ¹¹¹Cd used for measuring the hyperfine interaction with the EFG. Figure 1 shows the PAC time spectra $R(t)$ and their Fourier transforms $F(\omega)$ detected at ¹¹¹In-doped nano-ZnO. After annealing at 373 and 423 K, the PAC spectra exhibit a broad frequency distribution, similar to samples that were not annealed. This shows that the ¹¹¹In atoms are incorporated in nonunique crystalline environments characterized by a distri-

^{a)}Electronic mail: thomas.agne@tech-phys.uni-sb.de

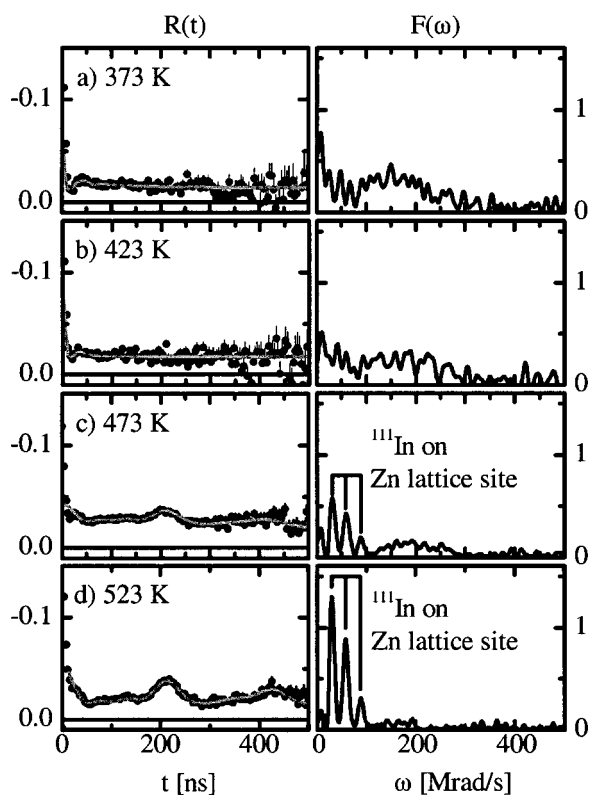


FIG. 1. PAC spectra of ^{111}In doped nano-ZnO after annealing between 373 and 523 K for 5 h by the hydrothermal method.

bution of EFG. After annealing at 473 K, an EFG characterized by $\nu_Q = 31(2)$ MHz and $\eta = 0.2$ is observed, whereby a fraction of about 12% of all ^{111}In atoms is situated in this environment. Increasing the annealing temperature to 523 K, this fraction increases to 25%. The coupling constant ν_Q of the observed EFG matches very well that of the EFG of ^{111}In on undisturbed Zn sites in bulk ZnO, mentioned earlier. The difference in the asymmetry parameter η of the observed EFG might indicate small distortions of the ZnO lattice in the environment of the ^{111}In atoms. These distortions might be caused by the incorporation of ^{111}In atoms near the surface of the crystallite or by internal strain present in the nanocrystallites. Lattice distortions in nanocrystallites are also known from extended x-ray absorption fine structure experiments.⁷

In order to investigate the response of the nano-ZnO host lattice to the hydrothermal treatment, undoped material was analyzed by XRD, TEM, optical absorption, and PL. For this purpose, a sample of nano-ZnO was divided into five parts in order to compare samples as prepared and after hydrothermal treatments at 373, 423, 473, and 523 K, respectively.

The XRD measurements were carried out using $\text{Cu K}\alpha$ radiation of a Siemens D-500 diffractometer in $\Theta-2\Theta$ geometry. The spectra plotted in Fig. 2 exclusively show the diffraction pattern of the hexagonal ZnO lattice. The line shape of the Bragg peaks was analyzed by the method of Warren/Averbach⁸ in order to yield size, size distribution, and microstrain of the nanocrystallites.⁹ After preparation, the nano-ZnO crystallites show a log-normal distribution with a median diameter $D_0 = 3.96$ nm, a geometrical standard deviation $\sigma = 1.11$, corresponding to a volume-weighted mean grain size of $\langle D \rangle_{\text{vol}} = 4.1$ nm, and a microstrain $\langle \epsilon^2 \rangle$

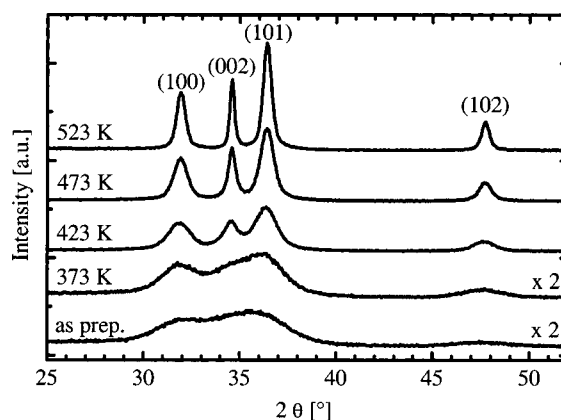


FIG. 2. XRD spectra of nano-ZnO as prepared and after hydrothermal treatment at different temperatures.

$= 1.50\%$. With increasing annealing temperature, the grain size and size distribution increase and reaches, at an annealing temperature of 473 K, the values $D_0 = 7.47$ nm and $\sigma = 1.5$, corresponding to $\langle D \rangle_{\text{vol}} = 11$ nm. At the same time, the microstrain decreases and disappears at 473 K, which coincides with the onset of the incorporation of the In atoms on regular Zn sites observed by PAC.

The grain size distribution and shape of the nano-ZnO crystallites was investigated by TEM using a JEM 2010 electron microscope. After preparation and after hydrothermal treatments at 373 and 423 K, the samples exhibit crystallites of spherical shape, and the distribution of the grain size matches well with the log-normal distribution of the XRD analysis. The sample annealed at 473 K still consists of nanocrystals of spherical shape but of few rod-shaped crystallites as well. After annealing at 523 K, the rod-shaped crystallites prevail, having a length up to 200 nm and a diameter of about 15 nm.

The optical absorption measurements were carried out using an UNICAM UV 500 spectrometer and nano-ZnO dissolved in 2-propanol. The spectra in Fig. 3 exhibit a blueshift due to the confinement effect. With increasing annealing temperature, the spectra show a shift of the band gap of nano-ZnO to smaller energies corresponding to the increase of the size of the nanocrystals observed by XRD and TEM. At the same time, the total absorption in the UV range increases with increasing annealing temperature up to 473 K,

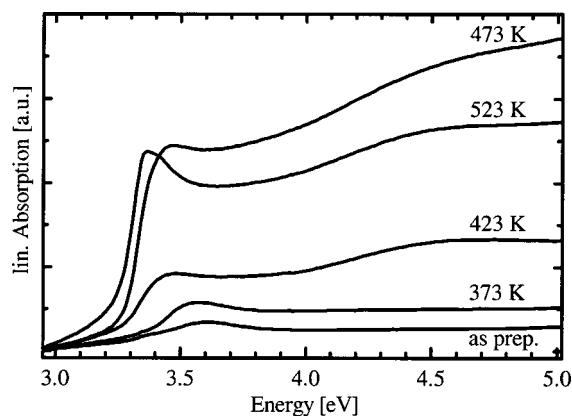


FIG. 3. Absorption spectra of nano-ZnO as prepared and after hydrothermal treatment at different temperatures. The spectra were recorded at room temperature.

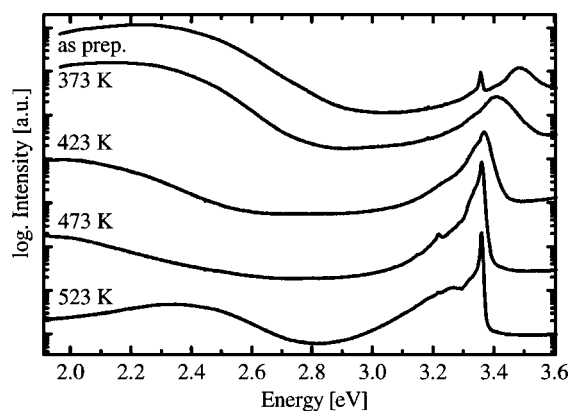


FIG. 4. PL spectra of nano-ZnO as prepared and after hydrothermal treatment at different temperatures. The spectra were recorded at 1.6 K and are shifted vertically for the sake of clarity.

indicating that an increasing fraction of nanocrystals is involved in the absorption process, possibly due to an ordering of the lattice of the ZnO nanocrystallites. The same results were obtained in case of hydrothermally treated nano-ZnO that was doped with ^{111}In .

The PL spectra were recorded at 1.6 K, using the 325-nm line of a HeCd laser for the excitation of the ZnO nanocrystals. The luminescence was analyzed by a 0.5 m grating monochromator and detected by a LN₂-cooled CCD camera. After preparation, in the UV range, the PL spectrum in Fig. 4 shows weak signals from a band–band recombination at 3.501 eV and a sharp line at 3.361 eV, which is almost in the energy range where excitons bound to neutral donors are observed in bulk ZnO.¹⁰ Thus, this line, assigned to a bound exciton, indicates the existence of donor-like defects in the nominally undoped nano-ZnO. In the visible range of this spectrum, a broad, deep emission band centered at 2.25 eV is present. For bulk ZnO, PL bands in this energy region are caused mainly by intrinsic structural defects like, for example, the green band centered at 2.4 eV, which is caused by oxygen vacancies.¹¹ After hydrothermal treatment at 373 and 423 K, the positions of the band–band recombination and the deep emission shift to lower energies, suggesting that the grain size of the nanocrystals increases and, at the same time, the intensity of the deep emission band decreases. After annealing at 473 K, the PL spectrum shows a strong, sharp line of bound excitons at 3.365 eV along with its LO-phonon replica.¹⁰ The deep emission band, now centered at 1.94 eV, is strongly reduced, indicating that the concentration of in-

trinsic defects causing this band is reduced. After annealing at 523 K, the line of bound excitons becomes still sharper but, at the same time, a new deep emission band arises, centered at 2.4 eV.

In summary, nano-ZnO with a mean grain size of 11 nm was successfully doped with the donor ^{111}In . The required incorporation of ^{111}In atoms on undisturbed Zn sites after hydrothermal treatment at 473 K was shown by detecting the site-specific EFG in nano-ZnO using PAC. The comparison with nano-ZnO that was annealed under vacuum in an oven shows the superiority of the hydrothermal process. At the same temperature of 473 K, the structural quality of nano-ZnO is significantly improved as revealed by TEM, XRD, absorption, and PL experiments. The results obtained by the different techniques indicate that the successful doping at 473 K is accompanied by the onset of crystal growth and might be due to the removal of intrinsic defects in the nanocrystallites. Based on the known conditions for the incorporation of ^{111}In atoms in nano ZnO, experiments with stable In atoms at relative concentrations of about 10^{-3} are in progress.

The authors are grateful to Manfred Schuler and Jörg Schmauch for performing the TEM experiments. The financial support by the DFG within the SFB 277 is gratefully acknowledged.

¹A. P. Alivisato, *Science* **271**, 933 (1996).

²M. Shim, C. Wang, D. J. Norris, and P. Guyot-Sionnest, *MRS Bull.* **26**, 1005 (2001).

³Th. Agne, Z. Guan, X. M. Li, H. Wolf, and Th. Wichert, *Phys. Status Solidi A* **229**, 819 (2002).

⁴A. Dierstein, H. Natter, F. Meyer, H.-O. Stephan, Ch. Kropf, and R. Hempelmann, *Scr. Mater.* **44**, 2209 (2001).

⁵Th. Wichert, in *Identification of Defects in Semiconductors*, edited by M. Stavola (Academic, London, 1999), p. 297.

⁶H. Wolf, S. Deubler, D. Forkel, H. Foettinger, M. Iwatschenko-Borho, F. Meyer, M. Renn, W. Witthuhn, and R. Helbig, *Mater. Sci. Forum* **10–12**, 863 (1986).

⁷J. Rockenberger, L. Tröger, A. Kornowski, T. Vossmeier, A. Eychmüller, J. Feldhaus, and H. Weller, *J. Phys. Chem. B* **101**, 2691 (1997).

⁸B. E. Warren and L. E. Averbach, *J. Appl. Phys.* **21**, 595 (1950); *J. Appl. Phys.* **23**, 497 (1952).

⁹H. Natter, M. Schmelzer, M.-S. Löffler, C. E. Krill, A. Fitch and R. Hempelmann, *J. Phys. Chem. B* **104**, 2467 (2000).

¹⁰Landolt/Börnstein, in *Numerical Data and Functional Relationships in Science and Technology—New Series III*, edited by U. Rössler (Springer, Berlin, 1999), Vol. 41B.

¹¹K. Vanheusden, W. L. Warren, C. H. Seager, D. R. Tallant, J. A. Voig, and B. E. Gnade, *J. Appl. Phys.* **79**, 7983 (1996).